Experimental Investigation of Steel Joist Design for Ductile Strength Limit State

JOSEPH ROBERT YOST, TIMOTHY J. HARRINGTON, JOSEPH J. POTE, SHAWN P. GROSS and DAVID W. DINEHART

ABSTRACT

Open web steel joists are prefabricated truss assemblies designed in accordance with specifications set forth by the Steel Joist Institute (SJI). Currently, the SJI design requirement is based on capacity, with no consideration for the governing-member strength limit state. The purpose of this research is to investigate a ductile design methodology for steel joists where the primary strength limit state is characterized by tension-member yielding and large inelastic deformation, followed by a secondary strength limit state of compression-member buckling. To achieve ductile behavior, a series of experimental joists were designed and manufactured using controlled over-strength ratios of relative member strengths so that tension-member yielding precluded compression-member buckling. The consequence of adjusting member strengths to induce ductile failure is a slight increase in joist weight. The experimental matrix consisted of 18 joist samples: six identical 33-ft-long K-series joists, six identical 33-ft-long LH-series joists and six identical 32-ft-long rod web joists. All joists were tested to collapse under simply supported uniform load conditions. Experimental results show that a ductile design is achievable because all 18 joists demonstrated tension-member yielding with significant deformation prior to a secondary limit state of compression-member buckling.

Keywords: steel joists, strength design, yielding, ductile limit state.

INTRODUCTION

Open web steel joists are prefabricated truss assemblies typically used in supporting roof and floor systems. The current specification for steel joist design is published by the Steel Joist Institute (SJI) and titled *Standard Specifications, Load Tables and Weight Tables for Steel Joists and Joist Girders,* 43rd edition (SJI, 2010). This specification is based on the 2005 AISC *Specification for Structural Steel Buildings*, ANSI/AISC 360-05, and has a dual format allowing either allowable stress design (ASD) or load and resistance factor design (LRFD). The strength limit state for steel joist members occurs by tension yield, compression buckling or interaction between axial force and bending moment. Presently, the SJI acknowledges four main joist types: K-series joists, longspan joists (LH-series), deep longspan joists (DLH-series) and joist girders. This paper explores the LRFD design methodology as related to design and behavior of K-series and LH-series joists.

In accordance with the current SJI design specifications, individual joist members are designed to meet strength requirements for a given design load combination. Using the LRFD design methodology, the member-strength design requirement may be expressed as follows:

$$\left\{ SR = \frac{f_u}{\phi F_n} \right\} \leq 1.0 \qquad (1)$$

In Equation 1, SR is member specific and defined as the stress ratio, f_u is the required strength or member stress resulting from external factored loads and ϕF_n is the design strength at the ultimate limit state. Both f_u and ϕF_n are defined for K-series joists and LH-series joists in Sections 4.2 and 103.2 of the SJI design specification, respectively (SJI, 2010). In effect, the SR is a measure of member efficiency, where $SR = 1.0$ indicates a member at its design capacity and $SR < 1.0$ indicates reserve strength.

Typically, joists are designed for economy so that individual design stress ratios of multiple tension and compression members are all simultaneously at or near 1.0. Therefore, no consideration is given by the SJI standard (2010) to controlling the member-strength capacity limit state, and ductile tensile yielding (of the bottom chord or tension web) is given no specified preference over sudden compressive

Joseph Robert Yost, Associate Professor, Department of Civil and Environmental Engineering, Villanova University, Villanova, PA (corresponding). Email: joseph.yost@villanova.edu

Timothy J. Harrington, Graduate Research Assistant, Department of Civil and Environmental Engineering, Villanova University, Villanova, PA. Email: tharri04@villanova.edu

Joseph J. Pote, Director of Research and Development, New Millennium Building Systems, LLC, Hope, AR. Email: Joe.Pote@newmill.com

Shawn P. Gross, Associate Professor, Department of Civil and Environmental Engineering, Villanova University, Villanova, PA. Email: shawn.gross@villanova.edu

David W. Dinehart, Professor, Department of Civil and Environmental Engineering, Villanova University, Villanova, PA. Email: david.dinehart@villanova.edu

Table 1. Design Conditions and Ductile Design Limits						
	Design Condition		Relative Strength Factor ρ_{max}		Slenderness Limit	
Member	K-Series	LH-Series	Existing	Ductile Design	Existing	Ductile Design
Bottom chord and end web	Axial tension		None	1.00	240	300
Top-chord interior panel less than 24 in.	Axial compression	Interaction		0.90	90	No change
Top-chord interior panel greater than 24 in.	Interaction					
Top-chord end panel					120	
Interior tension web	Axial tension			0.95	240	
Compression web	Axial compression			0.80	200	

buckling (of the top chord or compression web). As well, in truss design for non-seismic-load cases, the 2005 AISC *Specification* does not make specific reference to a preferred member-strength limit state. Importantly, the discussion here neglects connection-related limit states and is restricted to the member-level joist design, where the strength limit state will occur by tension-member yield or compression-member buckling. At the member level, research has shown that buckling of a steel joist compression member results in an instantaneous and significant loss in load bearing capacity (Yost et al., 2004, 2006). The authors suggest that, given this behavior, a joist designed for a ductile tensile-member yield limit state is desired over one with a sudden compression-member buckling limit state. In the event of severe overloads, the gradual yielding and deformation of a ductile element provides visual warning, load sharing to neighboring members and time for evacuation. Additionally, there is inherently less strength variance in components that are controlled by tensile yield limit state than those controlled by compression limit states, where force eccentricity, variability in end fixity and other variables contribute to less predictable buckling strengths. This characteristic was noted by Engelhardt et al. (2000) as related to strength and failure mode of experimental open web steel joists and by Rao et al. (2011) as related to strength and failure of lattice-type transmission towers.

The objective of this research study is experimental investigation of a steel joist design methodology where ductile tensile yielding is the intended primary-strength limit state. As the controlling tension member(s) yield, the load-bearing capacity of the joist remains intact. Ultimately, with sufficient inelastic deformation and in the absence of tensile fracture, the yield limit state is followed by a secondary strength limit state of compression-member buckling. At compression-member buckling, the joist strength is drastically reduced and ultimate collapse occurs. This paper outlines a design philosophy investigated with experimental testing of K-series and LH-series joists that have been designed for a ductile tensile yielding limit state. The focus of the study is exploratory, where experimental results are compared to predicted behavior in terms of load capacity and strength limit state mechanisms. From this comparison, conclusions are established regarding further pursuit of the proposed ductile methodology as related to steel joist design.

EXISTING SJI DESIGN REQUIREMENTS AND METHODOLOGY

Open-web steel joists are designed in accordance with SJI (2010), which has both LRFD and ASD methodologies. Design considerations not explicitly covered by SJI follow the AISC *Specification for Structural Steel Buildings* (AISC, 2005) or the AISI (American Iron and Steel Institute) *North American Specification for the Design of Cold-Formed Steel Structural Members* (AISI, 2007). LRFD is a probability-based philosophy that implements both load and resistance factors to ensure a minimal chance of inadequate capacity due to overload and/or understrength. This paper will focus solely on the LRFD methodology.

For K-series and LH-series joists, bottom chord and web members are designed for axial force only. Also, interior top chord panels of K-series joists that are less than 24 in. in length are designed for axial compression only. All other K-series and LH series top-chord panels must consider axial compression and bending interaction. Table 1 summarizes these design conditions for all members. The SJI (2010) LRFD design requirements for axial tension, axial compression and interaction are given in Equations 2 through 6 as follows:

$$\text{Axial tension:} \qquad \frac{P_u/A_g}{\phi_t F_y} \le 1 \tag{2}$$

Axial compression: $\frac{P_u/A_g}{\phi_c F_{cr}} \le 1$ (3)

Interaction at panel point: $\frac{f_{au}}{\phi_c F_y} + \frac{f_{bu}}{\phi_b F_y} \le 1$ (4)

Interaction at mid-panel:

for $\frac{f_{au}}{\phi F_{cr}} \ge 0.20$ $\frac{f_{au}}{\phi_c F_{cr}} + \frac{8}{9}\left[\frac{C_m f_{bu}}{\left(1-\frac{f_{au}}{\phi_c F_e}\right) Q\phi_b F_y}\right] \le 1.0$ (5)

for $\frac{f_{au}}{\phi F_{cr}} < 0.20$ $\frac{f_{au}}{2\phi_c F_{cr}} + \left[\frac{C_m f_{bu}}{\left(1-\frac{f_{au}}{\phi_c F_e}\right) Q\phi_b F_y}\right] \le 1.0$ (6)

The numerator terms of Equations 2 through 6 are LRFD required strength terms defined as:

P_u = factored axial force
M_u = factored bending moment
A_g = member cross-sectional area
S = minimum section modulus about axis of bending
f_{au} = factored axial compression stress = P_u/A_g
f_{bu} = factored bending stress = M_u/S
C_m = moment factor taken as
= $1 - 0.3f_{au}/\phi_c F_e$ for end panels
= $1 - 0.4f_{au}/\phi_c F_e$ for interior panels
F_e = Euler buckling stress = $\pi^2 E/(kL/r)^2$
F_y = yield stress assumed for design as 50 ksi
kL/r = maximum member slenderness
E = elastic modulus = 29,000 ksi

The denominator terms of Equations 2 through 6 are LRFD design strength terms and, for those not yet defined, are given as follows:

F_{cr} = $Q\left[0.658^{QF_y/F_e}\right]F_y$ for $kL/r \le 4.71\left(E/QF_y\right)^{1/2}$
= $0.877F_e$ for $kL/r > 4.71\left(E/QF_y\right)^{1/2}$
Q = reduction factor for slender compression elements
k = effective length factor
L/r = member slenderness
ϕ_t, ϕ_c, ϕ_b = resistance factors for tension, compression and bending, respectively
= 0.90

The effective length factor (k) is specified by the SJI specification (SJI, 2010) based on the joist series and member type. In addition to the design strength requirement identified in Equations 2 through 6, SJI also limits the maximum slenderness ratio (L/r) for the various member types. A summary of existing SJI design requirements as related to design condition and maximum slenderness is given in Table 1.

DUCTILE DESIGN PARAMETER AND METHODOLOGY

To design an open-web steel joist for a controlling, ductile tensile–yielding, strength limit state, the relative strengths of the individual members must be considered so that tension yielding precedes compression-member buckling. Thus, using the ductile design philosophy, the maximum stress ratio must be controlled by a tension member, and compression-member stress ratios must be sufficiently less to ensure yield before bucking. Accordingly, the relative strength factor (ρ) has been implemented to require minimum over-strength for all compression members (top chord and interior webs), as a function of the maximum member stress ratio. The relative strength relationship is given as:

$$\left\{\rho_i = \frac{(SR)_i}{(SR)_{\max}}\right\} \quad (7)$$

In Equation 7, ρ_i is the member relative strength factor, $(SR)_i$ is the corresponding member stress ratio and $(SR)_{max}$ is the maximum stress ratio for all members. Again, for a ductile design, $(SR)_{max}$ will be controlled by a tension member.

The stress ratios (SR) are as defined in Equation 1 and calculated using the procedures of Equations 2 through 6. Accordingly, as a structural system, the primary strength limit state of the joist will depend on the maximum relative strength factor for the tension and compression member groups. This relationship is shown in Table 2, where it is noted that to achieve a ductile limit state, $\rho < 1.00$ for all compression members and $\rho = 1.00$ for the maximum tension member. It is understood that these ρ limits are theoretical values, and the maximum ρ for all compression members will need to be less than 1.00 by a sufficient amount so that a tension yielding strength limit state is statistically probable. For this paper, the ρ factor is used in member selection and design of experimental joists so that ductile tensile yielding of end web or bottom chord is the primary strength limit state.

With regard to compression member over-strength, the aforementioned relative strength factor (ρ defined in Equation 7) is the primary design variable governing member selection and achievement of a ductile limit state. A ductile design is theoretically achieved by setting the relative strength factor for the compression members to some value less than 1.00, as noted in Table 2. The lower relative strength factor encourages a ductile limit state by providing additional strength to compression members. Statistically,

Table 2. Relative Strength Factor and Limit States			
	Member Group		
Relative Strength Factor	Compression	Tension	Primary Strength Limit State
ρ_{i-max}	< 1.00	= 1.00	Tensile yield
	= 1.00	= 1.00	Simultaneous tensile yield and compression buckling
	= 1.00	< 1.00	Compression buckling

the lower ρ factor on the compression members decreases their probability of failure. The maximum member relative strength factors used for design of experimental K-series, rod-web K-series and LH-series joists tested in this research, defined as ductile designs, are as follows:

- Bottom chord and end web members $\rho_{max} = 1.00$
- Interior tension webs $\rho_{max} = 0.95$
- Compression web members $\rho_{max} = 0.80$
- Top chord $\rho_{max} = 0.90$

The use of these values results in the prediction of bottom-chord or end-web tension yielding as the primary strength limit state, followed by top-chord buckling as the secondary strength limit state. Again, the relative strength factors are determined using Equation 7, with the stress ratios as given in Equation 1, and the selected members satisfy the proposed maximum relative strength limits. As part of the ductile design methodology, the maximum slenderness limit on end-web and bottom-chord tension members is increased from 240 to 300. The slenderness limit of 300 is consistent with the recommended maximum slenderness ratio for tension members in Section D1 of the 2005 AISC *Specification*. The ductile design parameter limits are summarized in Table 1.

From the maximum ρ factors noted, the compression web has the most reserve strength, with $\rho_{max} = 0.80$. The top chord, in comparison, has a smaller margin of relative over-strength, with $\rho_{max} = 0.90$. In selecting these values, it was considered that compression-web buckling is more variable than top-chord buckling, justifying the lower relative strength factor. The web-strength variability is due to the unsupported condition of the member length, variation in end fixity and eccentricity of axial load resulting from weld location and member alignment. In comparison, the top chord is typically continuously braced by the supporting deck, resulting in more predictable behavior. Also, the top chord is a continuous double-angle member, and size selection is generally controlled by the middle-panel stress ratio. For economy of the joist, top-chord selection is critical and excess over-strength is to be avoided. As well, the top-chord compression strength is known to be higher than that predicted using SJI procedures from research done by Iaboni et al. (2007) and Cianci et al. (2009). These results were all considered in setting the compression-web and top-chord ρ_{max} at 0.80 and 0.90, respectively, for design of the experimental joists. Future research may justify different ρ_{max} values for the compression members.

In conclusion, the proposed relative strength factors promote design of a joist with a high probability of tension member yielding and associated ductile limit state. Introducing a design parameter that regulates the respective strengths of compression and tension members resulted in the joist designs tested in this experimental study. Importantly, the ductile design procedure is offered as an exploratory exercise to investigate feasibility of the ductile design philosophy.

SAMPLE DETAILS AND EXPERIMENTAL PROGRAM

Experimental investigation included testing modified versions of three series of joists: K-series, LH-series and rod-web K-series, each designed per the ductile joist design procedure described earlier (and summarized in Table 1). For statistical validation, six identical samples were tested for each joist series. Figure 1 provides experimental load and support information, and Figure 2 provides sample details related to panel point layout and member sizes. The testing apparatus for all 18 joists was designed to simulate a uniformly distributed load on a simply supported span. Referring to Figure 1, the joists are loaded via four hydraulic cylinders, spaced 8 ft apart. The hydraulic load was manually pumped into the system and equally distributed to each of the four cylinders. As shown in detail A of Figure 1, each cylinder contacts a built-up load distribution unit that further distributes the load into eight point loads on the top chord at 1-ft spacing. The system applies 32 equal point loads, spaced at 1 ft on center, along the 32- or 33-ft length of the joist. Accordingly, the distributed force pattern, w, applied to the top chord is calculated as $w = P_{total}/32$ ft. The top chord was laterally braced at 2-ft intervals to prevent out-of-plane buckling. This combines with the multiple-point loads to simulate a uniformly loaded, continuously braced top-chord condition typical for joists. Additionally, the bottom chord

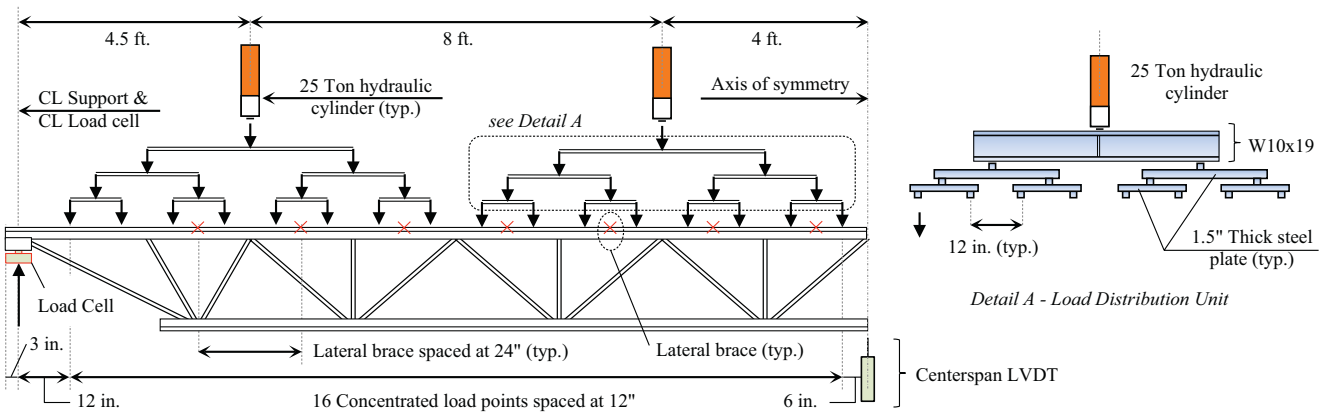

Fig. 1. Experimental load and support detail.

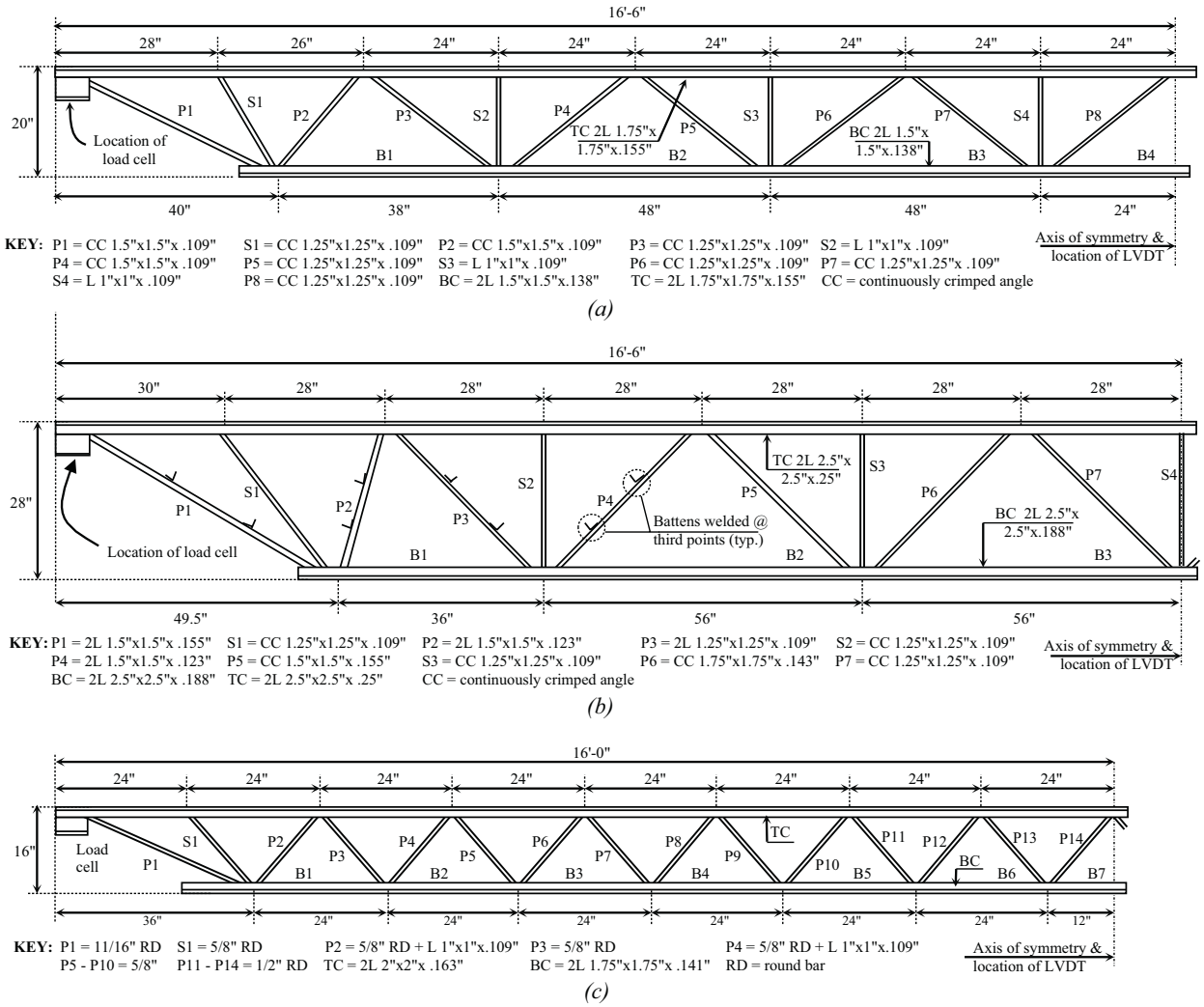

Fig. 2. Sample details: (a) typical K-series details (samples J1-1 through J1-6); (b) typical LH-series details (samples J2-1 through J2-6); (c) typical rod-web K-series details (samples J3-1 through J3-6).

Table 3. Sample Design Parameters and Failure Sequence								
			K-Series		LH-Series		Rod Web	
Member		ρ_{max} (–)	SR and ρ (–)	Predicted Strength Limit State Sequence	SR and ρ (–)	Strength Limit Sequence	SR and ρ (–)	Predicted Strength Limit State Sequence
Top Chord	End Panel	0.90	0.54		0.59		0.45	
	Interior Panel		0.87	Secondary	0.88	Secondary	0.87	Secondary
Bottom Chord		1.00	0.99	Primary	0.95		1.00	Primary
End Web	P1		1.00		1.00	Primary	0.92	
Interior Primary Web	P2	0.80	0.63		0.70		0.72	
	P3	0.95	0.63		0.81		0.43	
	P4	0.80	0.64		0.68		0.57	
	P5	0.95	0.40		0.54		0.36	
	P6	0.80	0.53		0.77		0.75	
	P7	0.95	0.24		0.66		0.28	
	P8	0.80	0.44				0.59	
	P12	0.80					0.77	

was braced at the third points to replicate transverse cross-bridging applied to joist systems. The bottom-chord center panels and both end webs were painted with lime wash to identify yielding during testing. During testing, load was applied at an approximate rate of 1,000 lb/min. Fifty-kip capacity load cells were placed at each support (Figure 1) to capture the total load applied to the system. A linear variable differential transducer (LVDT) recorded the deflection of the bottom chord at mid-span (Figure 1). Load and displacement were recorded at a sampling rate of 10 Hz using a 16-bit data acquisition system.

Sample details are shown in Figure 2. The K-series samples (Figure 2a) featured continuously crimped (CC), single-angle web members, which are characterized by bending the outermost region of each leg to fit and align the angle centroid in the same plane as the centroid of the chords. The larger LH-series samples (Figure 2b) featured a combination of continuously crimped, single-angle and double-angle web members. The rod-web K-series samples (Figure 2c) consisted of a continuous round bar bent at the panel points to form the web members. Also, the P2 and P4 compression webs were fabricated as rods reinforced with single angles, and the corresponding design strength for these reinforced members was used in determining the relative strength factors of Table 3.

All experimental joist samples were designed for a ductile limit state using an assumed yield strength (F_y) of 50 ksi and by the limiting relative strength factors described earlier (i.e., compression-web $\rho_{max} = 0.80$, top-chord $\rho_{max} = 0.90$, interior-tension web $\rho_{max} = 0.95$, bottom-chord and end-web $\rho_{max} = 1.00$). Table 3 presents maximum relative strength factors (ρ_{max}), member stress ratios (SR) and member relative strength factors (ρ) for the three joist series fabricated and tested in this study. For K-series samples, tensile yielding of both the bottom chord and end web is predicted as the relative strength factor for each at 1.00. This will be followed by top-chord buckling (ρ = 0.87). The controlling compression-web relative strength factor is 0.64 for member P4, so that web buckling is unlikely. For LH-series, ductile yielding of the end web is predicted (ρ = 1.00). Bottom-chord yielding (ρ = 0.95) could occur before achieving a secondary limit state of top-chord buckling (ρ = 0.88). Compression-web buckling is controlled by member P6 with ρ = 0.77 and is unlikely to occur before top-chord buckling. For the rod-web K-series joists, bottom-chord yielding is predicted (ρ = 1.00), followed by top-chord buckling (ρ = 0.87). Compression-web strength is controlled by P12 with ρ = 0.77. The over-strength on the compression web predicts top-chord buckling as the secondary limit state for the rod web joists.

The SJI-factored LRFD design loads determined by Equations 2 through 6 for the ductile joists detailed in Figure 2 are 418 lb/ft for the 20-in.-deep ductile K-series, 1303 lb/ft for the 28-in.-deep ductile LH-series and 420 lb/ft for the 16-in.-deep ductile rod-web K-series. In comparison to standard joists of equal span that are designed for the same factored loads but with no preference for controlling the strength limit state, the ductile joists weigh about 8% more. A significant amount of this weight increase is related to the top-chord size, where over-strength related to the design

limit of $\rho \leq 0.90$ requires a larger section. It should be understood, however, that the 8% weight increase noted is specific to the joists tested in this study and that, in general, the weight increase associated with the ductile design methodology will vary with many factors, such as span length, joist type, material availability and manufacturer.

The actual yield strength of the bottom-chord material was experimentally measured using the procedures of ASTM E8-04b, *Standard Test Methods for Tension Testing of Metallic Materials* (ASTM, 2004). For each of the 18 joists tested, a coupon was removed from the bottom-chord end panel. This location (bottom-chord end panel) was selected because of the low stress in this length. From test results, the average yield strength for the J1, J2 and J3 samples was found to be 60.3, 60.6 and 61.5 ksi, respectively. Thus, the measured yield strength is about 20% higher than was used for design. Significantly, unusually high yield strength may defeat the onset of tensile yield and ductile behavior. However, in the event of yield strength high enough to preclude the desired tensile yielding limit state, the use of relative over-strength factor, ρ, on the compression members would ensure strength in excess of a joist designed in accordance with SJI (2010).

TEST RESULTS

In preparation for testing to collapse, all joists were first preloaded to a nominal displacement of 1 in., or about 40% of the LRFD factored design load. This was done to ensure that all data acquisition was functioning properly and to seat the test sample in the loading frame, thereby removing any gap deformation among the loading apparatus, joist sample and supports. Upon release of the preload, the data acquisition system was zeroed and testing to failure commenced. Results for the K-series, LH-series and rod-web K-series are shown in Figure 3, where it is noted that the horizontal axis is center-span deflection and the vertical axis is the equivalent uniformly distributed load (w) determined as the total hydraulic force (P_{total}) divided by 32 ft ($w = P_{total}/32$ ft) Also, the load axis in Figure 3 includes the dead weight of the testing apparatus and self-weight of the joist, which are simply added to the force applied by the hydraulic cylinders. The total dead load was determined by weighing all components of the system in the absence of hydraulic force.

As can be seen from Figure 3, initial response for all joists is elastic with a linear load-deflection response, indicating all member stresses below yield. For each of the three joist

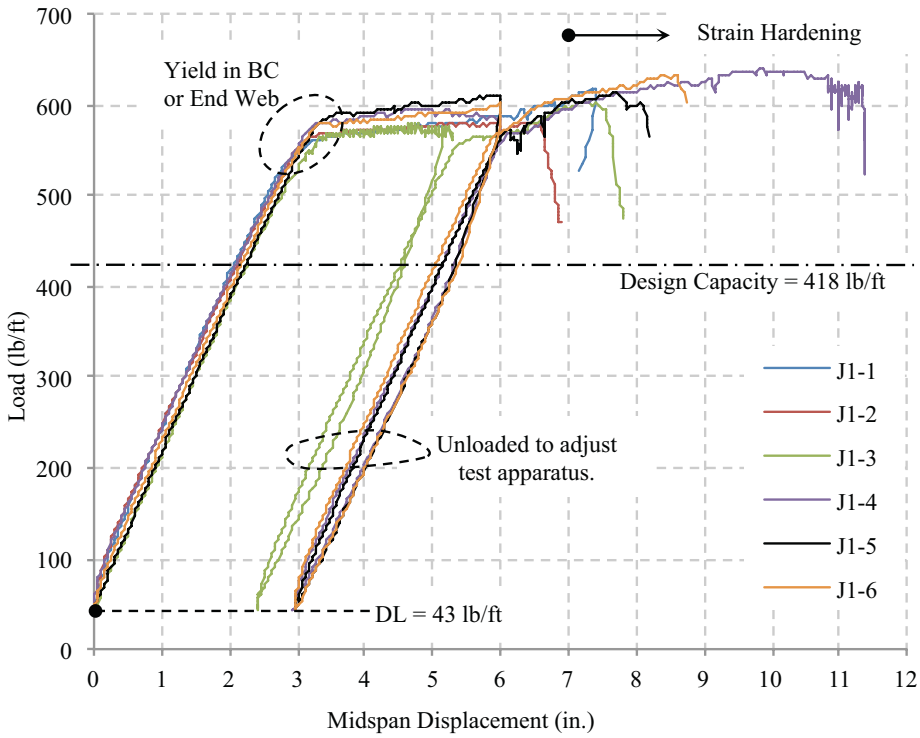

(a) K-Series

Fig. 3. Load-displacement results: (a) K-series (continued next page).

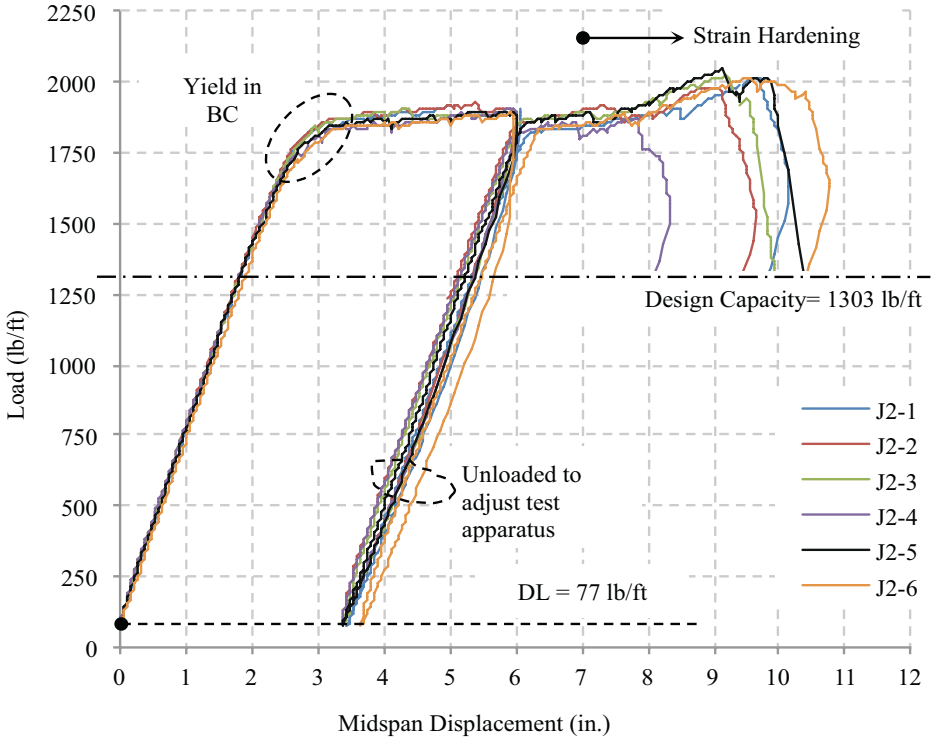

(b)

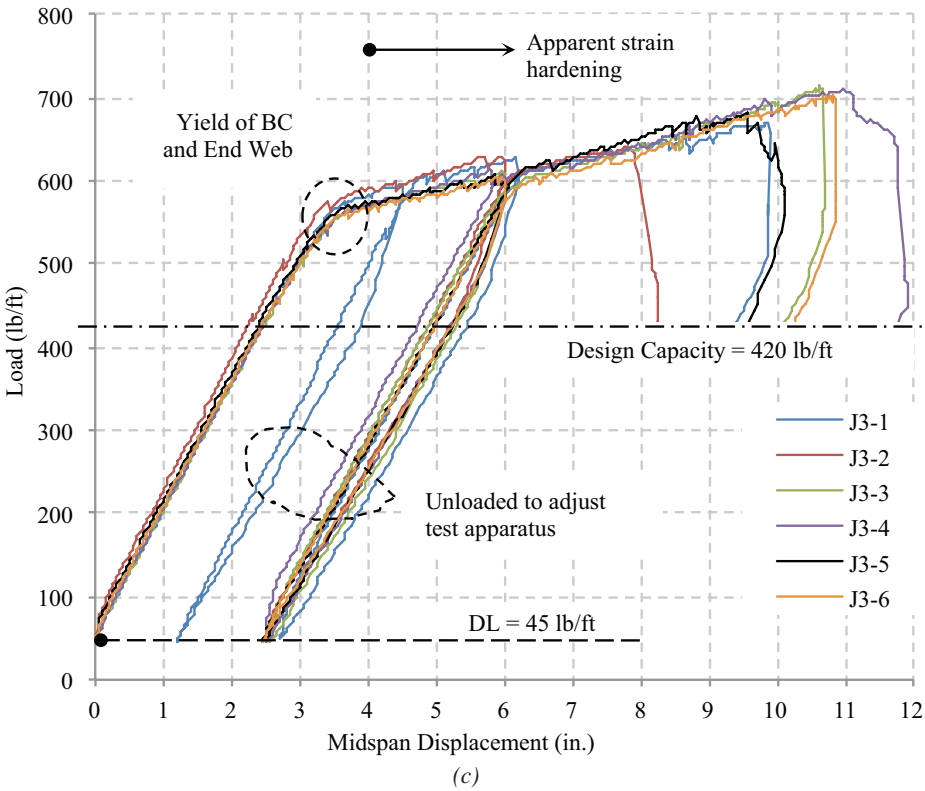

(c)

Fig. 3 continued. Load-displacement results: (b) LH-series; (c) rod-web K-series.

series, a high degree of repeatability is evident among the six identical samples. As the extreme fiber stress of the critical tension member reaches yield, the behavior transitions from elastic to inelastic, as is evident in the accelerated deflection rate and curvature of the load-deflection response. For all joist specimens, first yield occurred at the bottom-chord mid-span location and was visually identified by flaking of lime wash at that location. Typical bottom-chord yielding and lime-wash flaking can be seen in Figure 4a. Eventually, the critical tension member fully yields, and a plastic load plateau is achieved on the load-deflection response. For K-series and rod-web K-series, yielding of the end web was also detected, as shown in Figure 4b. No end-web yield was detected in the LH-series samples.

Following the fully plastic condition, all joists were loaded to approximately 6 in. of deflection and subsequently unloaded. The residual deflection is noted in Figure 3 and ranges from about 2.5 to 3.5 in. Unloading at 6 in. of deformation was necessary to reset the LVDT to a lower position and capture the full deformation of the joist, which would otherwise exceed the LVDT stroke capacity. The joists were then reloaded, resuming the load plateau and continued plastic deformation. Stiffness of the reloading branch was nearly identical to stiffness of the initial elastic response. All joists were loaded to collapse, which occurred by compression-member buckling of either the top chord or a web member. Table 4 summarizes test results in terms of load and displacement at yield (Y), plastic (P) and ultimate (U), as well as the secondary strength limit state and various ratios. In Table 4, yield (Y) is taken at initial departure from linear-elastic behavior; plastic (P) is defined as the load plateau, which is taken at 4 in. of joist displacement; and ultimate (U) is the secondary strength limit state of compression-member buckling. Figure 5 presents results graphically in terms of ultimate-displacement-to-yield-displacement or ductility ratio (Figure 5a) and average load ratios at yield, plastic and ultimate relative to the ductile design capacity (Figure 5b). Individual series results are discussed in the following sections.

K-Series Discussion (Samples J1-1 through J1-6)

The predicted failure mode for these joists is given in Table 3 and expected to be simultaneous yielding of the end web and bottom chord (ρ = 0.99 and 1.00), followed by top-chord buckling (ρ = 0.87). The failure behavior observed during testing is consistent with this prediction. As mentioned, flaking of lime wash, indicating yielding, was observed on the bottom-chord and end-web members. Bottom-chord yielding was observed to initiate adjacent to the panel points of the bottom-chord mid-span segment (B4). As inelastic displacement increased, the bottom chord yielded region spread down the length of panel B4 (Figure 4d). At ultimate load capacity, the complete cross-section of the bottom-chord B4 panel for the entire member length showed evidence of yielding; however, no yield was detected in the neighboring bottom-chord panels (B3 and B5). End-web yielding generally occurred after significant bottom-chord yielding and was evident over approximately the middle half of both end-web members.

After significant plastic deformation, each sample experienced top chord buckling. In general, top-chord buckling occurred between brace points and about the *y*-axis, or out of the plane of the joist, characterized by an unrecoverable drop in load-carrying capacity. A typical top-chord buckling condition is shown in Figure 4c. For sample J1-2, the load distribution unit was rotated out-of-plane, inducing an eccentric load on the top chord and promoting premature buckling. Thus, strength and deformation at ultimate of this sample are not considered in Table 4. For samples J1-1, J1-4 and J1-6, there appears to be a region of strain hardening after approximately 7 in. of deflection (Figure 3a). This is evident in the slight increase in load after the plastic load plateau.

Excluding sample J1-2, deformation at ultimate ranged from 7.37 in. (sample J1-1) to 10.8 in. (sample J1-4). In terms of span length, this represents $L/54$ to $L/37$, a tremendous amount of deformation. Ductility results in Table 4 and Figure 5a show a range from 2.47 (sample J1-5) to 3.55 (sample J1-4) with a series average of 2.83, demonstrating a significant amount of energy dissipation in the form of inelastic deformation. Average strength ratios in Figure 5b show progressively increasing capacity at yield, plastic and ultimate relative to design, and strength ratio standard deviations are all very low (Table 4). Specifically, the yield-strength-to-design-strength ratio (Y/D in Table 4 and Figure 5b) ranges from 1.23 to 1.34, with a series average of 1.29, and ultimate-strength-to-design-strength ratio (U/D in Table 4 and Figure 5b) ranges from 1.45 to 1.52, with a series average of 1.49. The strength ratios and associated standard deviations indicate predictable behavior with low variability, conservative design relative to the primary strength limit state of tensile yield and substantial reserve strength relative to the secondary strength limit state of compression buckling.

LH-Series Discussion (Samples J2-1 through J2-6)

The predicted strength limit state for these joists is given in Table 3 and expected to be end-web yielding (ρ = 1.00) followed by secondary buckling of the top chord (ρ = 0.88). The bottom chord has a ρ of 0.95 and may yield prior to a compression-member buckling. The observed behavior was not consistent with this prediction. Rather, in all six cases, yielding occurred on the bottom chord only, initiating on either side of the mid-span panel point, as shown in Figure 4e. Bottom chord yielding was observed simultaneously in both members adjacent to the mid-span panel point (B3 and B4). As deformation increased, bottom-chord yielding

Table 4. Summary of Test Results

		Yield (Y)		Plastic (P)		Ultimate (U)			Ratio P/Y		Ratio U/Y		Design Load Ratio[b]		
Series	Sample	Load (lb/ft)	Disp. (in.)	Load (lb/ft)	Disp. (in.)	Secondary Strength Limit State[a]	Load (lb/ft)	Disp. (in.)	Disp. (–)	Load (–)	Disp. (–)	Load (–)	Y/D (–)	P/D (–)	U/D (–)
K-Series	J1-1	515	2.67	568	4.00	TCB	620	7.37	1.50	1.10	2.76	1.20	1.23	1.36	1.49
	J1-2	538	2.90	574	4.00	LAC			1.38	1.07			1.29	1.38	
	J1-3	512	2.86	567	4.00	TCB	604	7.40	1.40	1.11	2.59	1.18	1.23	1.36	1.45
	J1-4	559	3.04	589	4.00		634	10.8	1.32	1.05	3.55	1.13	1.34	1.41	1.52
	J1-5	557	3.12	592	4.00		614	7.72	1.28	1.06	2.47	1.10	1.34	1.42	1.47
	J1-6	558	3.08	582	4.00		634	8.57	1.30	1.04	2.78	1.14	1.34	1.39	1.52
	Average	540	3.00	579	4.00		621	8.37	1.36	1.07	2.83	1.15	1.29	1.39	1.49
	Std. Dev.	22	0.17	11	0.00		13	1.44	0.08	0.03	0.42	0.04	0.05	0.03	0.03
LH-Series	J2-1	1670	2.43	1878	4.00	TCB	2019	9.62	1.65	1.12	3.96	1.21	1.28	1.44	1.55
	J2-2	1671	2.41	1882	4.00	TCB & S4B	1982	9.03	1.66	1.13	3.75	1.19	1.28	1.44	1.52
	J2-3	1721	2.54	1886	4.00	TCB	2026	9.19	1.57	1.10	3.62	1.18	1.32	1.45	1.56
	J2-4	1648	2.40	1852	4.00		1864	7.82	1.67	1.12	3.26	1.13	1.27	1.42	1.43
	J2-5	1640	2.41	1868	4.00	TCB & S4B	2013	9.83	1.66	1.14	4.08	1.23	1.26	1.43	1.55
	J2-6	1617	2.43	1855	4.00	TCB	2004	9.86	1.65	1.15	4.06	1.24	1.24	1.42	1.54
	Average	1661	2.44	1870.2	4.00		1985	9.23	1.64	1.13	3.79	1.20	1.28	1.44	1.52
	Std. Dev.	36	0.05	14.43	0.00		61	0.77	0.03	0.02	0.32	0.04	0.03	0.01	0.05
Rod-web K-Series	J3-1	523	3.12	582	4.00	PWB	667	9.89	1.28	1.11	3.17	1.28	1.25	1.39	1.59
	J3-2	541	3.09	589	4.00	TCB	638	7.82	1.29	1.09	2.53	1.18	1.29	1.40	1.52
	J3-3	512	3.10	567	4.00	PWB	709	10.65	1.29	1.11	3.44	1.39	1.22	1.35	1.69
	J3-4	518	3.14	568	4.00	TCB	703	11.08	1.27	1.10	3.53	1.36	1.23	1.35	1.68
	J3-5	531	3.18	572	4.00	PWB	679	9.54	1.26	1.08	3.00	1.28	1.26	1.36	1.62
	J3-6	539	3.35	566	4.00	PWB	698	10.86	1.19	1.05	3.24	1.29	1.28	1.35	1.66
	Average	527	3.16	574	4.00		682	9.97	1.27	1.09	3.15	1.30	1.26	1.37	1.63
	Std. Dev.	12	0.10	9	0.00		27	1.21	0.04	0.02	0.36	0.07	0.03	0.02	0.06

[a] LAC = load apparatus complication, TCB = top-chord buckling, S4B = S4 web buckling, PWB = primary web buckling

[b] LRFD Factored Design Load (D) K-series = 418 lb/ft, LH-series = 1303 lb/ft, Rod-web K-series = 420 lb/ft

spread down the length of the B3 and B4 panels. However, no end-web yielding occurred in any of the samples. The LH-series end webs are double-angle members with battens welded to the third points. The end webs did not yield as predicted, possibly due to a higher yield strength than the bottom chord. At approximately 7.0 in. of deformation, a region of strain hardening occurred (Figure 3b) where the load capacity gradually increased until ultimate collapse under the secondary strength limit state of compression-member buckling.

The secondary strength limit state for samples J2-2 and J2-5 was a combination of buckling of the S4 web member followed by buckling of the top chord at center span. The S4 web buckling was not a sudden condition, rather a deformed bent shape of the member was evident as the joist approached failure by top-chord buckling, as is shown in Figure 6a. The deformed shape of the S4 web only occurred at very high deflection, in excess of approximately 7 in. At ultimate collapse, top-chord buckling was out of the plane of the joist for sample J2-2. For sample J2-5, top-chord buckling occurred in the plane of the joist between the two panel points located 28 in. on either side of center span. Simultaneous buckling of the S4 member was also observed, which resulted in the loss of in-plane bracing by the S4 web at center span on the top chord. This behavior is shown in Figure 6b. For the remaining four LH-series samples, some evidence of S4 buckling or bending was observed; however, ultimate collapse occurred by top-chord buckling out of the plane of the joist at an interior panel.

The S4 member is a secondary vertical web member and is not predicted by elastic analysis to be highly stressed by direct application of externally applied loads. The elastic analysis is based on relatively small deformations where the S4 member force is largely based on tributary loading, as is shown in Figure 7a. Secondary web members are generally not important force-resisting members, but rather primarily provide in-plane bracing for the top chord. However, considering its location at the highly stressed top-chord

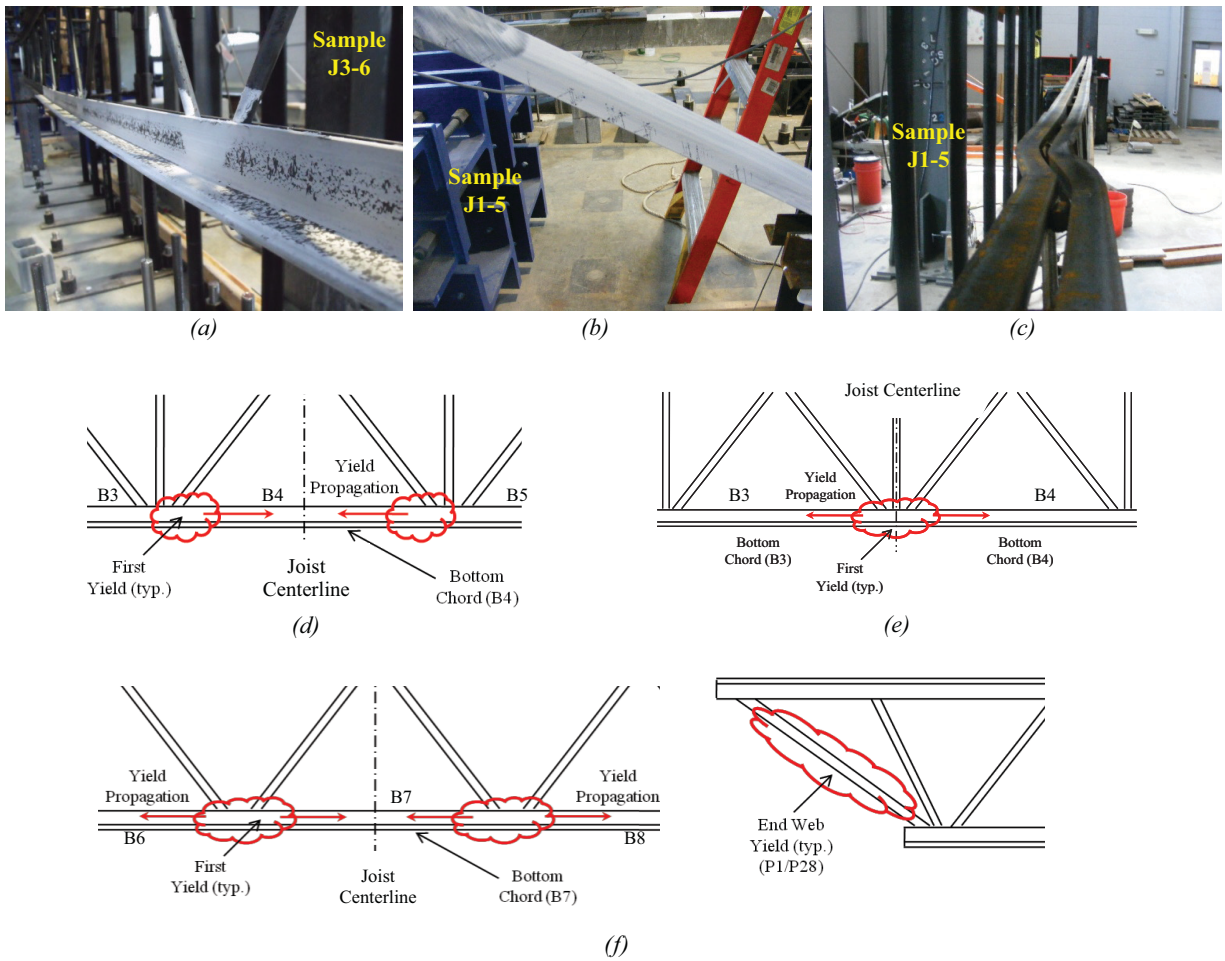

Fig. 4. Member yielding and buckling: (a) bottom-chord yielding; (b) end-web yielding; (c) top-chord buckling; (d) bottom-chord yielding in K-series samples; (e) bottom-chord yielding in LH-series samples; (f) bottom-chord and end-web yielding in rod-web K-series samples.

mid-panels, test results show that the S4 member appears to become highly stressed under extreme inelastic joist displacement. This condition likely results from the very large vertical deformation and corresponding development of a vertical force component in the top-chord axial force that, by joint equilibrium, acts on the vertical web, as shown in Figure 7b. This results in stresses well beyond those calculated for elastic behavior and small deformations. Currently, the SJI requires only that vertical web members be designed for gravity load plus 0.5% of the top-chord axial force (SJI, 2010). This requirement should be reexamined with consideration of ensuring that vertical-web members possess the necessary strength required to resist axial forces associated with large deformation behavior. It should be noted that this behavior was only evident after the test joists had successfully demonstrated the intended goal of extreme inelastic ductile deformation while retaining full load-bearing capacity and that the vertical web buckling was not sudden in nature.

Ductility results of Table 4 and Figure 5a show that the LH-series achieved the highest performance of the three series tested. Ductility ranged between 3.26 (sample J2-4) and 4.08 (sample J2-5), with a series average of 3.79. The high ductility ratios appear to result in a strain-hardening region that begins at approximately 7 in. of deformation, approximately three times the yield displacement. At these high deflections, strain hardening in the yielding tension member is achieved, resulting in the tangent stiffness apparent in the test results. This strain hardening behavior is further supported by the load-strain results for sample J2-6 shown in Figure 8, where strain data were collected at the middle length of both end webs, as well as the bottom chord

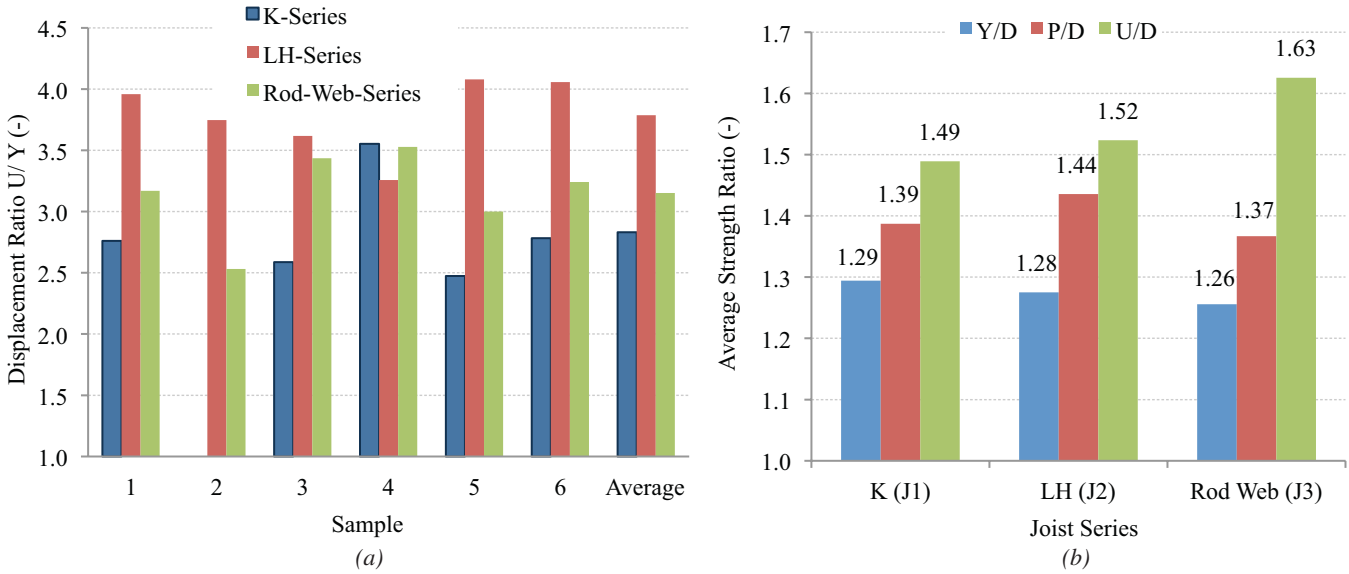

Fig. 5. Ratio results (a) ductility ratio; (b) average strength ratios.

Fig. 6. Secondary limit state failure for J2 and J3 series: (a) sample J2-2; (b) sample J2-5; (c) sample J3-1; (d) sample J3-5.

at center span. Figure 8 shows that the end webs remained elastic (SG1, SG2, SG5, SG6), but there is severe yielding in the bottom chord (SG3, SG4). The strain at yield is measured to be about 2,100 microstrain, after which there is a sharp transition to a perfectly plastic condition. At about 16,000 microstrain, strain hardening initiates and continues to about 19,500 microstrain, at which point secondary compression-member buckling occurs. After testing, the bottom chords were all visually inspected and measured with a digital caliper, and there was no visible or measurable evidence of a reduced cross-section or necking.

Average strength ratios in Figure 5b show progressively increasing capacity at yield, plastic and ultimate relative to design and also indicate strength ratio standard deviations are all very low (Table 4). The yield-strength-to-design-strength ratio (Y/D in Table 4 and Figure 5b) ranges from 1.24 to 1.32, with a series average of 1.28, and ultimate-strength-to-design-strength ratio (U/D in Table 4 and Figure 5b) ranges from 1.43 to 1.56, with a series average of 1.52. As with the K-series joists, strength ratios and associated standard deviations indicate predictable behavior with low variability, conservative design relative to the primary

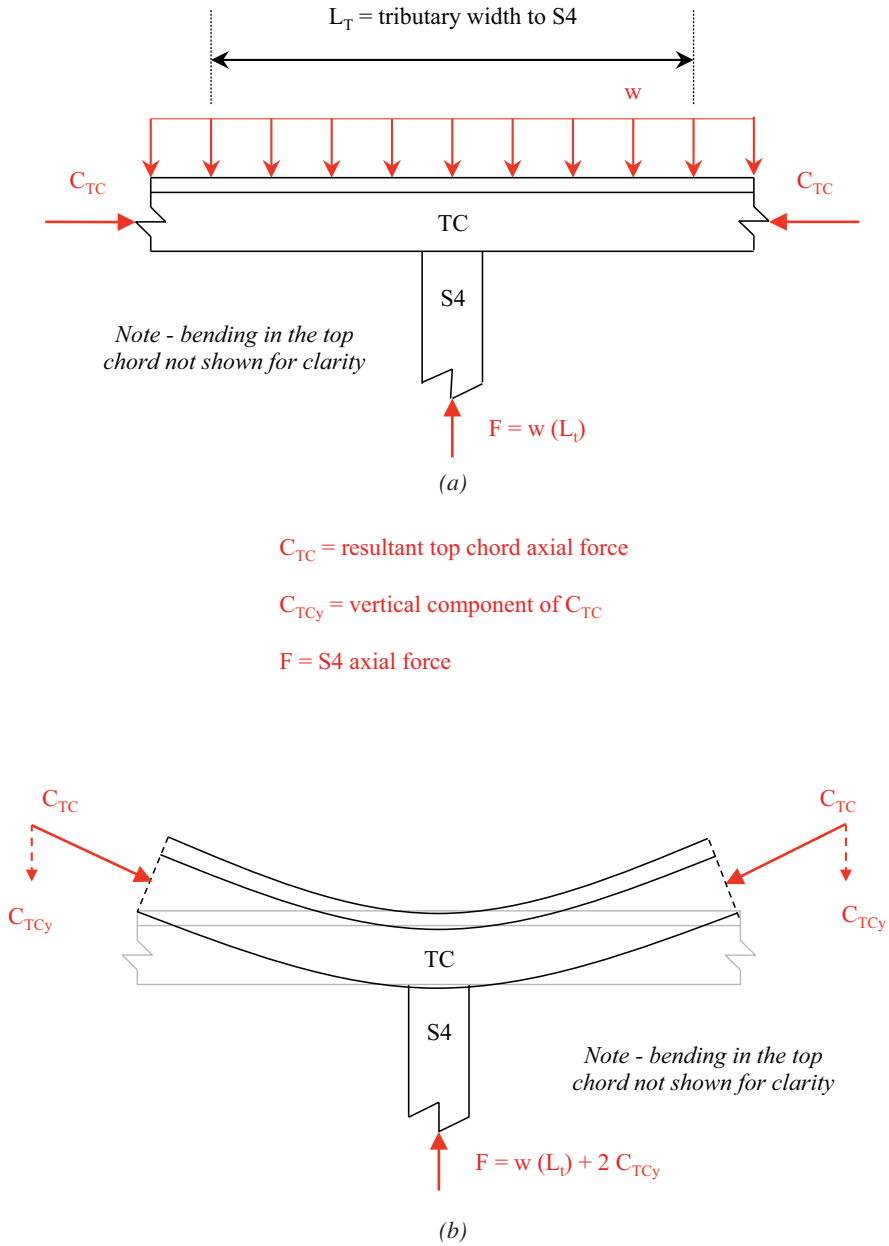

Fig. 7. S4 member axial force: (a) small deformation; (b) large deformation.

strength limit state of tensile yield and substantial reserve strength relative to the secondary limit state.

Rod-Web K-Series Discussion (Samples J3-1 through J3-6)

The predicted strength limit state sequence for these joists as provided in Table 3 is bottom-chord yielding ($\rho = 1.00$) followed by top-chord buckling ($\rho = 0.87$). Yielding of the end web before top-chord buckling is possible with $\rho = 0.92$. The load-deflection results for the rod-web K-series joists are shown in Figure 3c, where extreme ductile behavior is noted. For all samples, response is initially elastic followed by bottom-chord yielding. The observed yielding result is consistent with predicted behavior. In all cases, first yielding occurred in the bottom-chord mid-span panel (B7). This mechanism was observed to start adjacent to the panel points on each side of the B7 panel, as is shown in Figure 4f. As inelastic displacement increased, yielding spread down the length of the B7 panel as well as into adjacent bottom-chord panels (B6 and B8). At very high displacements, lime-wash flaking was also observed in the B5 and B9 panels. After the onset of bottom-chord yielding, end-web yielding was also observed. In some instances, the end-web yielding was observed over the entire cross-section and length of the end bars (Figures 4f and 6c).

After full, bottom-chord yielding, the behavior appears to directly enter a strain-hardening region (Figure 3c). This is evident in the absence of a horizontal load plateau following full yielding of the bottom chord. Rather, there is an immediate resumption of load increase, albeit at a much reduced rate. The load versus displacement plot of Figure 3c shows an inclined yield plateau, indicating an increase in strength as deflections increase. This behavior was attributed to strain hardening after about 7 in. of deflection in the K-series and LH-series joists (Figures 3a and 3b); however, for the rod-web K-series, its onset is immediate and continuous throughout the loading from first yield to ultimate collapse. This appears to be the result of more numerous rod-web members relative to the geometric layout of deeper joists. With the spacing between panel points minimized, the stress redistribution can occur more continuously as the bottom-chord member is yielding.

At secondary limit state, only two of the six joists (J3-2 and J3-4) experienced the top-chord buckling anticipated by the theoretical failure sequence. The top-chord buckling locations were confined to the central panels (T7 through T10). Three specimens (J3-1, J3-3, J3-6) collapsed in buckling of the first interior compression web member (P2/P27), which is a ⅝-in.-round bar reinforced with a 1 in. × 1 in. × 0.109 in. angle. In each of these cases, the buckled web member was adjacent to an end web member that demonstrated substantial yielding prior to buckling. These types of failure are shown in Figure 6c. The J3-5 specimen had a relatively unique secondary limit state of buckling in the P8/P21 and P6/P23 compression web members, as shown in Figure 6d. While not necessarily expected, their ultimate buckling is understandable in that they are the first unreinforced compression bars from the end of the joist and have design stress ratios of 0.59 and 0.75, respectively.

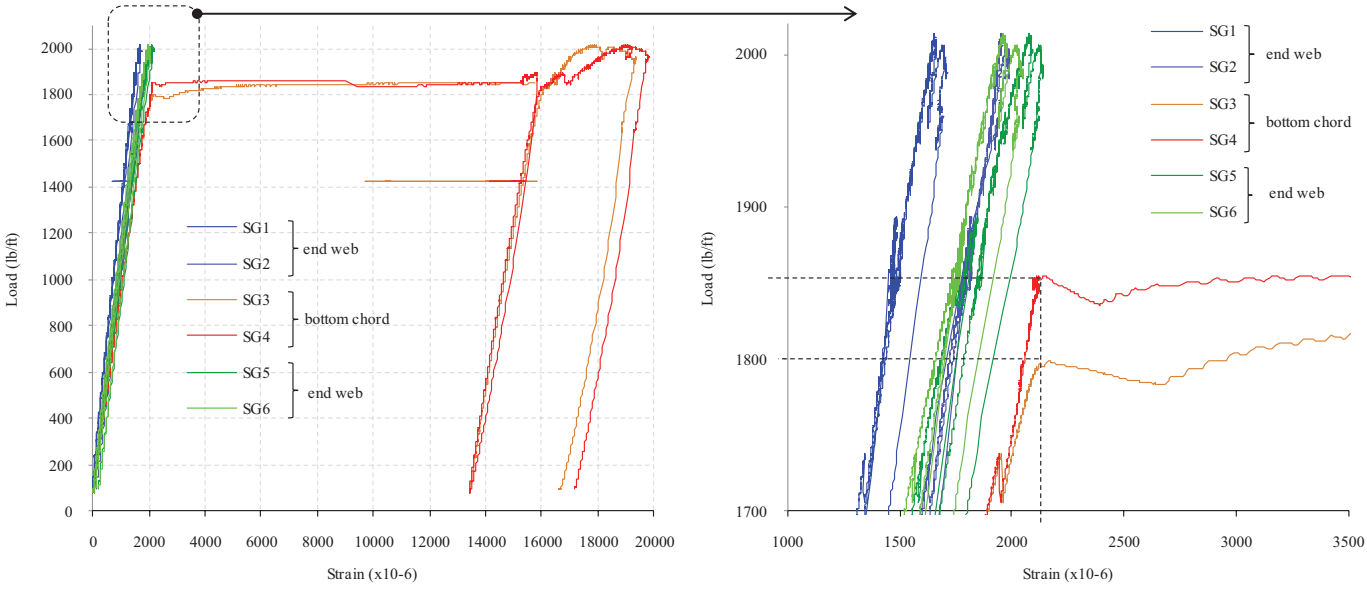

Fig. 8. Tension-member strain results for sample J2-6.

Ductility ratios from Figure 5a range from 2.53 for sample J3-2 to 3.53 for sample J3-4, with a series average of 3.15. As with J1 and J2 samples, average strength ratios in Figure 5b show progressively increasing capacity at yield, plastic and ultimate relative to design, and strength ratio standard deviations are all very low (Table 4). The yield-strength-to-design-strength ratio (Y/D in Table 4 and Figure 5b) ranges from 1.22 to 1.29, with a series average of 1.26, and ultimate-strength-to-design-strength ratio (U/D in Table 4 and Figure 5b) ranges from 1.52 to 1.69, with a series average of 1.63. The strength ratio U/D is the highest of the three joist series tested, and represents additional strength developed from the post-yield inclined load plateau (Figure 3c). As with the K-series and LH-series joists, strength ratios and associated standard deviations indicate predictable behavior with low variability, conservative design relative to the primary strength limit state of tensile yield and substantial reserve strength relative to the secondary limit state.

DISCUSSION OF TEST RESULTS AND RELABILITY INVESTGATION

The ductile design methodology related to controlling member strength by implementation of the relative strength factor ρ in member selection (all as summarized in Table 1) is fully supported by 18 experimental data points.

For each joist tested, the intended ductile behavior was achieved and characterized by tension yield, followed by significant plastic deformation and ultimate failure by compression buckling. Thus, the ρ factors selected for design provided sufficient compression-member over-strength, allowing tensile yield as the initial strength limit state and, importantly, yield and ultimate collapse at strengths well in excess of the predicted design capacity. As well, the experimental test results are uniquely significant when measured relative to the design limit state (D) at each the yield (Y) or primary strength limit state, plastic limit state (P) and ultimate (U) or secondary strength limit state conditions. That is, experimental behavior is characterized by three unique limit states that occurred sequentially with increasing strength capacity in all 18 samples (Figure 5b). Ultimately, these three limit states (Y, P and U) are a predictable sequence, where the plastic limit state represents an important transition from the primary to the secondary strength limit states. Strength ratios and corresponding statistical data are important in this discussion as well. As is seen in Table 4 and Figure 5b, the strength ratios at each of the yield, plastic and ultimate conditions relative to LRFD ductile design capacity are progressively increasing, with each ratio having a significant factor of safety and low standard deviation. This ensures a conservative design with the primary strength limit state corresponding to the yield limit condition, significant residual strength at the secondary limit state and low variability for all three strength ratios.

Although an in-depth reliability study is beyond the scope of this paper, the reduced variance in the strength of members in tension relative to the strength of slender members in compression results in improved reliability and is worth exploring as an extension of the test results presented. If materials purchased for the bottom chord and end webs are limited to a specific steel alloy supplied by a specific mill, further reductions in variance can be found, resulting in more reliable strength and limit state control. Accordingly, an exploratory reliability investigation has been performed based on the tested joist plastic strengths (P), together with merchant bar steel mill test data, and employing the criteria and assumptions used to develop the 2005 AISC LRFD design approach. Merchant bar steel mill test data have been furnished by Steel Dynamics Roanoke Bar Division, for ASTM A529-50 steel, covering a time frame from May 2008 to October 2012 (Steel Dynamics, 2012). In all, the data included 11,546 test samples representing 4,337 batches of steel. The yield stress population distribution and statistical data for these 11,546 samples are provided in Figure 9. For joist test strength ratios, the 18 tested joist plastic strengths have been divided by the joist experimental design strength, which is defined as the nominal strength times the ratio of member tested F_y to specified minimum F_y (50 ksi). A summary of these loads and ratios is provided in Table 5. Lacking data for broad comparisons of actual section properties to nominal section properties, the industry standard data published in Table F1 of AISI 2007 (AISI, 2007) have been used for these ratios.

The LRFD design approach used by both the 2005 AISC *Specification* and the 2007 AISI design specification follows the equations and procedures presented in a series of eight articles in the September 1978 issue of the *Journal of the Structural Division*. However, the two differ in the ratio of live-to-dead loads used for calibration of LRFD to the historical ASD design method. For LRFD calibration, the 2005 AISC *Specification* uses a live-to-dead load ratio of 3, whereas AISI uses a live-to-dead load ratio of 5. From AISI Chapter F, *Tests for Special Cases,* and Commentary on Chapter A, *General Provisions*, the relative reliability index is calculated as:

$$\beta = \frac{\ln\left[\frac{C_\phi}{\phi}(M_m F_m P_m\right]}{\sqrt{V_M^2 + V_F^2 + C_P V_P^2 + V_Q^2}} \tag{8}$$

where

β = relative reliability index
ρ = resistance factor = 0.90
C_ϕ = calibration coefficient, which may be shown [using procedures demonstrated in AISI (2007) Commentary on Chapter A, *General Provisions*] to equal 1.481 for LRFD with live-to-dead load ratio of 3

M_m = mean value of material factor, M
= 1.135 from Steel Dynamics Roanoke Bar Division data for ASTM A529-50 merchant bar (see Figure 9)
F_m = mean value of fabrication factor, F
= 1.0 from AISI (2007) Table F1
P_m = mean value of professional factor, P, for tested component
= 1.033 from test-average-plastic-to-experimental-design ratio (see Table 5)
V_M = coefficient of variation of material factor
= 0.0602 from Steel Dynamics Roanoke Bar Division data for ASTM A529-50 merchant bar (Figure 9)
V_F = coefficient of variation of fabrication factor
= 0.05 from AISI 2007 Table F1
C_P = correction factor
= 1.196 for 18 test samples
V_P = coefficient of variation of joist test results
= 0.029 from test results data (see Table 5)
V_Q = coefficient of variation of load effect, which may be shown (using procedures demonstrated in AISI (2007) Commentary on Chapter A, *General Provisions*) to equal 0.187 for LRFD with live-to-dead load ratio of 3

Substitution of these values into Equation 8 yields an approximate plastic strength $\beta = 3.2$. This is an improved reliability as compared to the approximate $\beta = 2.6$ for members, reported in the 2005 AISC *Specification* and reflective of expectations of a joist designed in accordance with the SJI standard (2010). It should be noted that the calculated approximate plastic strength $\beta = 3.2$ is based on the joist tested plastic limit state (Tables 4 and 5), above which the joists demonstrated consistent reserve capacity before attaining ultimate maximum load capacity.

In summary, the ductile design methodology employed in this experimental program produced the predicted behavior related to achieving ductile failure, resulting in a slow collapse mechanism characterized by large inelastic deformation and improved reliability. The loss in economy is acknowledged as a consequence of adjusting member strengths.

CONCLUSIONS AND FINDINGS

The research presented in this study experimentally explores a design methodology for open-web steel joists, where the primary strength limit state is ductile tensile yielding of the bottom chord or end web, which, after significant inelastic

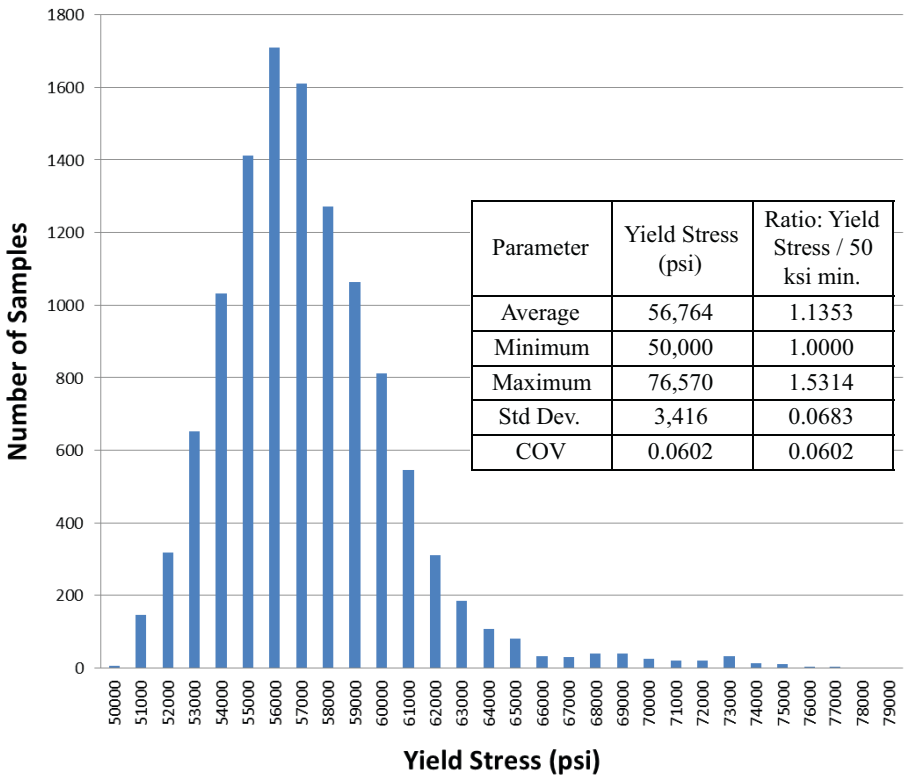

Parameter	Yield Stress (psi)	Ratio: Yield Stress / 50 ksi min.
Average	56,764	1.1353
Minimum	50,000	1.0000
Maximum	76,570	1.5314
Std Dev.	3,416	0.0683
COV	0.0602	0.0602

Fig. 9. Yield stress population distribution and statistical data.

Table 5. Statistical Data for Joist Tests						
Series	**Sample**	**SJI LRFD Design Load (lb/ft)**	**F_y Experimental (ksi)**	**Experimental Design Load (lb/ft)**	**Plastic Strength (lb/ft)**	**Ratio Plastic/ Exp Design Load (–)**
K-Series	J1-1	418	60.3	560	568	1.01
	J1-2				574	1.02
	J1-3				567	1.01
	J1-4				589	1.05
	J1-5				592	1.06
	J1-6				582	1.04
LH-Series	J2-1	1303	60.6	1755	1878	1.07
	J2-2				1882	1.07
	J2-3				1886	1.07
	J2-4				1852	1.06
	J2-5				1868	1.06
	J2-6				1855	1.06
Rod-web K-Series	J3-1	420	61.5	574	582	1.01
	J3-2				589	1.03
	J3-3				567	0.99
	J3-4				568	0.99
	J3-5				572	1.00
	J3-6				566	0.99
All	Average					1.0330
	Std. Dev.					0.0302
	COV					0.0293
	Quantity					18

deformation, is followed by a secondary strength limit state of buckling of the top chord or compression web. Importantly, the study scope is restricted to gravity loading of simply supported K-series and LH-series joists, where the bottom chord and end webs are in tension and the top chord is in compression. For other load and support conditions, where the force sense in these members is different, the stated findings may not apply.

Ductile behavior was achieved by adjusting the relative design strengths of the individual tension and compression members so that tension yielding precedes compression-member buckling. Adjusting the individual member tension and compression strengths to the appropriate relative strength factors results in a predictable failure sequence characterized by ductile behavior and sufficient capacity to support SJI LRFD design loads. The proposed ductile design methodology was experimentally investigated in the design, manufacturing and testing of modified K-series, LH-series and rod-web K-series joists. For each joist series, six identical joists were tested, for a total of 18 tests. All joists were simply supported with a uniformly distributed loading pattern applied to the top chord. The lengths were either 32 or 33 ft, and the top chord was laterally braced at 2-ft intervals. The following conclusions are derived from the test results:

- All 18 joists behaved in a ductile fashion, as predicted, with tension yielding as the primary strength limit state followed by compression-member buckling as the secondary strength limit state. For K-series and rod-web K-series joists, both the bottom chord and end web experienced tension yielding. For the LH-series joists, only the bottom chord experienced yielding.

- For the joists tested in this research, implementation of the ductile design relative strength factors as the basis for member selection resulted in an 8% increase in weight as compared to a conventionally designed joist of equal span and capacity. In general, the weight increase

associated with implementation of the ductile design methodology will vary with many factors such as span length, joist type, material availability and manufacturer.

- The yield strength for all 18 samples exceeded the LRFD design strength by a significant amount. For K-series, LH-series and rod-web K-series joists, the six sample average yield loads were 1.29, 1.28 and 1.26 times the LRFD design load, respectively. Reference for this conclusion is made to Table 4 and Figure 5b. This indicates a conservative design relative to the primary yield strength limit state.

- The series average ultimate strength ratio, which is defined as the load at ultimate divided by the LRFD factored design load, is 1.49, 1.52 and 1.63 for K-series, LH-series and rod-web K-series joists, respectively. Reference for this conclusion is made to Table 4 and Figure 5b. This indicates substantial reserve strength relative to the secondary strength limit state.

- The average ductility ratio for six identical samples, which is defined as the deflection at ultimate divided by the deflection at yield, was 2.83, 3.79 and 3.15 for K-series, LH-series and rod-web K-series joists, respectively. For all 18 samples tested, this ratio ranged from 2.47 to 4.08. Reference for this conclusion is made to Figure 5a and Table 4.

- The relative reliability factor calculated using joist test results and statistical data from 11,546 merchant bar test samples was 3.2, an increase of 23% over the 2.6 used by current SJI LRFD methodology. Reference for this conclusion is made to Figure 9 and Table 5.

- For the K-series and LH-series joists, the yield limit state was followed by a horizontal load plateau. After significant deformation, the load plateau terminated, and these joists experienced a gradual increase in load capacity that is associated with strain hardening in the yielded tension member. Reference for this conclusion is made to Figures 3 and 8. Ultimate collapse occurred as a secondary limit state of buckling of the top chord or compression web.

- For rod-web K-series joists, the yield limit state was followed by an immediate resumption of increasing load-bearing capacity. The post-yield behavior was an inclined linear increase in loading until secondary compression failure. Ultimate collapse occurred as a secondary limit state of top-chord buckling or compression-web buckling. Reference for this conclusion is made to Figure 3c.

- In several of the LH-series joists, bending and buckling of the secondary S4 web at mid-span was observed. This occurred after very high inelastic deformation and is attributed to development of a vertical component to the resultant chord axial force that delivers a substantial compression force on the web. Reference for this conclusion is made to Figures 6a, 6b and 7.

In conclusion, the ductile design philosophy was successfully implemented using the relative strength factor (ρ) as the basis for member selection, ensuring sufficient compression member over-strength relative to tension-member yield strength.

ACKNOWLEDGMENTS

The authors are grateful to Commercial Metals Company Inc. for providing financial support and materials for this project and to Steel Dynamics Roanoke Bar Division for sharing statistical data from mill tests of ASTM A529-50 merchant bar. The authors also wish to thank the Villanova University Office of Research and Sponsored Projects for providing graduate tuition support and the Villanova University Center for Undergraduate Research and Fellowships for supporting an undergraduate researcher on this project.

SYMBOLS

A_g	= gross cross-sectional area
C_m	= moment factor
C_{TC}, C_{TCy}	= top-chord resultant force and vertical force component, respectively
C_P, C_ϕ	= correction factor and calibration coefficient, respectively
E	= elastic modulus
f_{au}	= factored axial stress
f_{bu}	= factored bending stress
f_u	= required member stress
F	= axial force in S4 web member
F_{cr}	= critical buckling stress
F_e	= Euler buckling stress
F_n	= nominal member stress at ultimate
F_y	= yield stress
F_m, M_m, P_m	= mean value of fabrication factor, material factor and professional factor, respectively
k	= effective length factor
L	= member length
L_t	= tributary length to top-chord panel point
M_u	= factored bending moment
P_u	= factored axial force
Q	= local buckling reduction factor
r	= radius of gyration
S	= section modulus
SR	= stress ratio
V_M, V_F, V_P, V_Q	= coefficients of variation for material, fabrication, joist test results and load effect, respectively
w	= applied distributed force pattern
β	= relative reliability index
ϕ	= strength reduction factor
ρ	= relative strength factor

REFERENCES

AISC (2005), *Specifications for Structural Steel Buildings,* 13th ed., American Institute of Steel Construction, Chicago, IL.

AISI (2007), *North American Specification for the Design of Cold-Formed Steel Structural Members*, American Iron and Steel Institute, Washington, DC.

ASTM (2004), "E8-04b Standard Test Methods of Tension Testing of Metallic Materials," ASTM E8-04b, American Society of Testing and Materials, West Conshohocken, PA.

Cianci, P.A., Yost, J.R., Gross, S.P. and Dinehart, D.W. (2009), "Design and Behavior of Ductile Open Web Steel Joists: Phase II," Research Report, Commercial Metal Corporation, Hope, AR.

Engelhardt, M.D., Kates, Z., Beck, H. and Stasney, B. (2000), "Experiments on the Effects of Power Actuated Fasteners on the Strength of Open Web Steel Joists," AISC, *Engineering Journal*, Fourth Quarter.

Iaboni, N.J., Yost, J.R., Gross, S.P. and Dinehart, D.W. (2007), "Design and Behavior of Ductile Open Web Steel Joists," Research Report, Commercial Metal Corporation, Hope, AR.

Rao, N., Knight, S., Seetharaman, S., Lakshmanan, N. and Iyer, N. (2011), "Failure Analysis of Transmission Line Towers," *Journal of Performance of Constructed Facilities*, May/June.

SJI (2010), *Standard Specifications, Load Tables, and Weight Tables for Steel Joists and Joist Girders,* 43rd ed., Steel Joist Institute, Myrtle Beach, SC.

Steel Dynamics (2012), "Internal Quality Control Report," Steel Dynamics Corporation, Roanoke, VA.

Yost, J.R., Dinehart, D.W., Gross, S.P., Pote, J. and Gargan, B. (2004) "Strength and Design of Open Web Steel Joists with Crimped-End Web Members," *Journal of Structural Engineering*, Vol. 130, No. 5.

Yost, J.R., Dinehart, D.W., Gross, S.P., Pote, J. and Deeney, J. (2006), "Buckling Strength of Single Angle Compression Members in K-Series Joists," *Engineering Journal,* second quarter.